Ferrocenyl-Based π-Conjugated Complexes: Modulation of Electronic Properties by Symmetric/Asymmetric Cyclopentadienyl Substitution

Demis Paolucci,* Massimo Marcaccio, Carlo Bruno, Dario Braga,* Marco Polito,* and Francesco Paolucci*

Dipartimento di Chimica "G. Ciamician", Università degli Studi di Bologna, Via Selmi 2, 40126 Bologna, Italy

Fabrizia Grepioni†

Dipartimento di Chimica, Università di Sassari, Via Vienna 2, 07100 Sassari, Italy

Received October 12, 2004

The electronic properties of the family of pyridyl− and pyrimidyl− ferrocenyl complexes [Fe(η^5-C_5H_4-4-C_5H_4N)(η^5-C_5H_5)] (**1**), [Fe(η^5-C_5H_4-4-C_5H_4N)$_2$] (**2**), [Fe(η^5-C_5H_4-4-C_5H_4N)(η^5-C_5H_4-5-$C_4H_3N_2$)] (**3**), [Fe(η^5-C_5H_4-5-$C_4H_3N_2$)$_2$] (**4**), [Fe(η^5-C_5H_4−C_6H_4-4-C_5H_4N)(η^5-C_5H_4-5-C_5H_4N)] (**5**), and [Fe(η^5-C_5H_4−C_6H_4-4-C_5H_4N)$_2$] (**6**), prepared by Suzuki coupling starting from ferrocenyl diboronic acid, have been investigated by electrochemical, spectroscopic, and quantum-chemical methods. All complexes display photo- and electrochemical stability and strong electronic interactions in the ground state between the ferrocenyl moiety and pyridine/pyrimidine rings. The efficient modulation of the potentials of ferrocenyl-based oxidation is shown to be strongly dependent on the nature of the hetero ring. These features, together with their high chelating ability, are potentially useful in the preparation of redox-active *complexes of complexes* such as mixed-metal metallamacrocycles.

Introduction

The development and investigation of photo- and/or electroactive supramolecular systems are of high current interest. The major goals are the design, assembly, and evaluation of new materials to be exploited as push−pull systems,[1] molecular switches,[2] logic gates,[3] and systems based on intramolecular charge transfer.[4] In this context, the choice of suitable bridging ligands in the communication among metal centers is of prime importance.

Recently, we reported the synthesis and structural characterization by solid-state techniques of a series of mono- and disubstituted pyridine/pyrimidine ferrocenyl complexes, obtained either by coupling in solution[5a] or by mechanochemical treatment[5b] of solid reactants. In this work we expand on these results by investigating the electrochemical and spectroscopic behavior of the conjugated ferrocene derivatives represented in Chart 1: [Fe(η^5-C_5H_4-4-C_5H_4N)(η^5-C_5H_5)] (**1**), [Fe(η^5-C_5H_4-4-C_5H_4N)$_2$] (**2**), [Fe(η^5-C_5H_4-4-C_5H_4N)(η^5-C_5H_4-5-$C_4H_3N_2$)] (**3**), [Fe(η^5-C_5H_4-5-$C_4H_3N_2$)$_2$] (**4**), [Fe(η^5-C_5H_4−C_6H_4-4-C_5H_4N)(η^5-C_5H_4-5-C_5H_4N)] (**5**), and [Fe(η^5-C_5H_4−C_6H_4-4-C_5H_4N)$_2$] (**6**). The π-conjugated donor systems, formed by the metal-coordinated cyclopentadienyl ligand and its aromatic substituents, associated with the good electron donor capability of ferrocene,[4e] are expected to show a wide variety of electrochemical and spectroscopic properties that, combined with the good coordinating ability of the pyridine and/or pyrimidine rings, may be exploited in the preparation of *complexes of complexes*, whereby the complexes are, in their turn, used as ligands. Indeed, the compound [Fe(η^5-C_5H_4-4-C_5H_4N)$_2$]

* To whom correspondence should be addressed. Fax: +39 0512099456; Tel: +39 0512099465. E-mail: demis.paolucci@unibo.it (D.P.); francesco.paolucci@unibo.it (F.P.); dario.braga@unibo.it (D.B.).

† Present address: Dipartimento di Chimica "G. Ciamician", Università degli Studi di Bologna, Via Selmi 2, 40126 Bologna, Italy. E-mail: fabrizia.grepioni@unibo.it.

(1) (a) Long, N. J. *Angew. Chem., Int. Ed. Engl.* **1995**, *34*, 21. (b) Zyss, J.; Ledoux, I.; Volkov, S.; Chernyak, V.; Mukamel, S.; Bartholomew, G. P.; Bazan, G. C. *J. Am. Chem. Soc.* **2000**, *122*, 11956. (c) Lee, J. Y.; Kim, K. S.; Mhin, B. J. *J. Chem. Phys.* **2001**, *115*, 9484. (d) Green, M. L.; Marder, S. R.; Thomson, M. E.; Bandy, J. E.; Bloor, D.; Kolinsky, P. V.; Jones, R. J. *Nature* **1987**, *330*, 360. (e) Jayaprakash, K. N.; Ray, P. C.; Matsuoka, I.; Bhadbhade, M. M.; Puranik, V. G.; Das, P. K.; Nishihara, H.; Sarkar, A. *Organometallics* **1999**, *18*, 3851.

(2) (a) Balzani, V.; Juris, A.; Venturi, M.; Campagna, S.; Seroni, S. *Chem. Rev.* **1996**, *96*, 759. (b) de Silva, A. P.; McClenaghan, N. D.; McCoy, C. P. *Molecular Switches*; Wiley-VCH: New York, 2000, pp 339−361. (c) Jiao, J.; Long, G. J.; Grandjean, F.; Beatty, A. M.; Fehlner, T. P. *J. Am. Chem. Soc.* **2003**, *125*, 7522. (d) Rambidi, N. G. *Microelectron. Eng.* **2003**, *69*, 485. (e) Miyaji, H.; Collinson, S. R.; Prokes, I.; Tucker, J. H. R. *Chem. Commun.* **2003**, 64.

(3) (a) de Silva, P. A.; McClenaghan, N. D. *Chem. Eur. J.* **2004**, *10*, 574. (b) Credi, A.; Balzani, V.; Langford, S. J.; Stoddart, J. F. *J. Am. Chem. Soc.* **1997**, *119*, 2679.

(4) (a) Guldi, D. M.; Marcaccio, M.; Paolucci, D.; Paolucci, F.; Tagmatarchis, N.; Tasis, D.; Vázquez, E.; Prato, M. *Angew. Chem., Int. Ed.* **2003**, *42*, 4206. (b) Guldi, D. M.; Imahori, H.; Tamaki, K.; Kashiwagi, Y.; Yamada, H.; Sakata, Y.; Fukuzumi, S. *J. Phys. Chem. A* **2004**, *108*, 541. (c) Campielli, S.; Vàzquez, E.; Milic, D.; Prato, M.; Barberá, J.; Guldi, D. M.; Marcaccio, M.; Paolucci, D.; Paolucci, F.; Deschenaux, R. *J. Mater. Chem.* **2004**, *14*, 1266. (d) Carano, M.; Cicogna, F.; D'Ambra, I.; Gaddi, B.; Ingrosso, G.; Marcaccio, M.; Paolucci, D.; Paolucci, F.; Pinzino, C.; Roffia, S. *Organometallics* **2002**, *21*, 5583. (e) Hubig, S. M.; Kochi, J. K. In *Electron Transfer in Chemistry*; Balzani, V., Ed.; Wiley-VCH: Weinheim, Germany, 2001; Vol. 2, pp 618−676, and references cited therein.

(5) (a) Braga, D.; Polito, M.; Bracaccini, M.; D'Addario, D.; Tagliavini, E.; Sturba, L.; Grepioni, F. *Organometallics* **2003**, *22*, 2142. (b) Braga, D.; Polito, M.; D'Addario, D.; Grepioni, F. *Organometallics* **2004**, *23*, 2810. (c) Braga, D.; Polito, M.; D'Addario, D.; Tagliavini, E.; Proserpio, D. M.; Grepioni, F.; Steed, J. W. *Organometallics* **2003**, *22*, 4532.

10.1021/om049212l CCC: $30.25
Publication on Web 02/15/2005

Chart 1

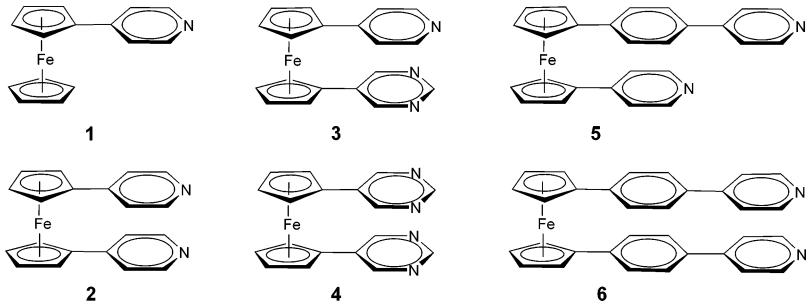

(**2**) has been already utilized in the preparation of a series of heterometallamacrocycles by reaction with Cu(II), Cd(II), Zn(II), and Ag(I) salts.[5c]

In the following we report the results of an investigation of complexes **1**−**6**, carried out by cyclic voltammetry (CV), electronic absorption spectroscopy, and spectroelectrochemistry. The experimental results were complemented by molecular orbital (MO) calculations at the density functional theory (DFT) level. The combination of theory and experiment has afforded an unequivocal localization of redox processes within the molecular structure and a better understanding of mutual interactions among redox centers.

Experimental Section

Syntheses. The ferrocenyl complexes **1**−**6** were prepared as reported previously,[5] starting from ferrocene-1,1′-diboronic acid, $[Fe(\eta^5\text{-}C_5H_4B(OH)_2)_2]_4$,[6] and from Br-pyridine/pyrimidine in the presence of a catalytic amount of $PdCl_2$[1,1′-bis-(diphenylphosphino)ferrocene], through a Suzuki coupling protocol. While all reactions were carried out in solution, compounds **2** and **4** were also obtained quantitatively by carrying out same reactions under solvent-free conditions by mechanical treatment of solid reactants.

The salt ferrocenium tetrafluoroborate, $[Fe(\eta^5\text{-}C_5H_5)_2][BF_4]$, was synthesized as reported elsewhere.[7] Since this salt rapidly degrades in organic solvents, $[Fe(\eta^5\text{-}C_5H_5)_2][PF_6]$ was precipitated by adding an excess of KPF_6 to an aqueous solution of $[Fe(\eta^5\text{-}C_5H_5)_2][BF_4]$. After the mixture was stirred for 10 min and allowed to stand for a further 10 min, the blue solid was filtered, washed with a small amount of water, and finally dried in air.

Electrochemistry. All materials were reagent grade chemicals. The supporting electrolyte tetrabutylammonium hexafluorophosphate (TBAH, from Fluka) was used as received. Ultra-dry tetrahydrofuran (udTHF) from NanoClust (Bologna, Italy) was chosen as solvent, due to the widest potential windows. The cell, containing the supporting electrolyte and the electroactive compound, was dried under vacuum at 370 K for at least 48 h. Afterward the solvent was distilled by a trap-to-trap procedure into the electrochemical cell just before performing the electrochemical experiment. The pressure measured in the electrochemical cell prior to performing the trap-to-trap distillation of the solvent was typically around 1×10^{-5} mbar.

The one-compartment electrochemical cell was of airtight design, with high-vacuum glass stopcocks fitted with either Teflon or Kalrez (DuPont) O-rings, to prevent contamination by grease. The connections to the high-vacuum line and to the Schlenk flask containing the solvent were made by spherical joints fitted with Kalrez O-rings. Also, the working electrode consisted of a Pt-disk ultramicroelectrode (with diameter of 125 μm), sealed in glass. The counter electrode consisted of a platinum spiral, and the quasi-reference electrode was a silver spiral. The quasi-reference electrode drift was negligible for the time required by a single experiment. Both the counter and reference electrodes were separated from the working electrode by ∼0.5 cm. Further details about the electrochemical cell were described elsewhere.[8] Potentials were measured with the ferrocene or decamethylferrocene standards and are always referred to the saturated calomel electrode (SCE). $E_{1/2}$ values correspond to $(E_{pc} + E_{pa})/2$ from cyclic voltammetry (CV), whereas for irreversible processes the peak potential E_p is measured at 1 V s^{-1}. Ferrocene (decamethylferrocene) was also used as an internal standard for checking the electrochemical reversibility of a redox couple. Voltammograms were recorded with a custom-made fast potentiostat[9] controlled by an AMEL Model 568 function generator. Data acquisition was performed by a Nicolet Model 3091 digital oscilloscope interfaced to a PC. The minimization of ohmic drop was achieved through the positive feedback circuit implemented in the potentiostat. DigiSim 3.0 software (Bioanalytical Systems Inc.) was used for digital simulation of CV curves.

Spectroelectrochemistry and Electronic Absorption Spectra. UV−vis spectroelectrochemical experiments were carried out using a quartz OTTLE (optically transparent thin-layer electrode) cell with a 0.03 cm path length and a reservoir area attached to the top to hold reference and counter electrodes. Temperature control was achieved by a special cell holder with quartz windows and two nitrogen flows (one at room temperature and the other at low temperature) independently regulated by two needle valves attached to two flow meters (Jencons, Item 3015-045). The temperature of the cuvette was monitored with a thermocouple connected to a CAL-9000 digital thermometer and can be tuned between room temperature and 230 K, with an accuracy better than ±0.2 K. The working electrode was a Pt−Rh (90:10) gauze with an optical transparency of about 40%. The counter electrode was a thick Pt wire, and a Ag/AgCl electrode, separated by a glass frit, was the reference electrode. All of the details concerning the spectroelectrochemical setup have been reported elsewhere.[10]

The potential was set using an AMEL Model 552 potentiostat connected to an AMEL Model 568 function generator.

The cell used to collect the electronic absorption spectra was a 0.2 and 0.1 cm path length quarz cuvette. All the spectra were recorded by a Varian Cary 5 UV−vis−near-IR spectrophotometer.

Results and Discussion

Electrochemical Properties. The electrochemical properties of complexes **1**−**6** were investigated by CV in THF solutions, under ultra-dry conditions.

(6) Knapp, R.; Rehahn, M. *J. Organomet. Chem.* **1993**, *452*, 235.
(7) Connelly, N. G.; Geiger, W. E. *Chem. Rev.* **1996**, *96*, 877.
(8) Marcaccio, M.; Paolucci, F.; Paradisi, C.; Carano, M.; Soffia, S.; Fontanesi, C.; Yellowlees, L. J.; Serroni, S.; Campagna, S.; Balzani, V. *J. Electroanal. Chem.* **2002**, *532*, 99.
(9) Amatore, C.; Lefrou, C. *J. Electroanal. Chem.* **1992**, *324*, 33.
(10) Lee, S. M.; Kowallick, R.; Marcaccio, M.; McCleverty, J. A.; Ward, M. D. *J. Chem. Soc., Dalton Trans.* **1998**, 3443.

Table 1. Electrochemical Potentials (vs SCE) of the Ferrocenyl Ligands[a]

compd	$E_{1/2}$/V				
Fc	0.58				−2.98[b]
1	0.68			−2.40	
2	0.76		−2.24		−2.77[c] (−2.64)
3	0.78		−2.22	−2.52	
4	0.79		−2.26[c] (−2.20)	−2.47[c] (−2.41)	
5	0.69	−2.12		−2.41	−2.87[c]
6	0.62	−2.11	−2.22	−2.56	−2.79[c]

[a] Data collected for a 0.7 mM solution, in 0.05 M TBAH/THF, at 1 V s^{-1} and 295 K. [b] Extrapolated from data recorded at 225 K. [c] E_p for quasi-reversible or totally irreversible behaviors, values in parentheses are $E_{1/2}$ values determined by digital simulation.

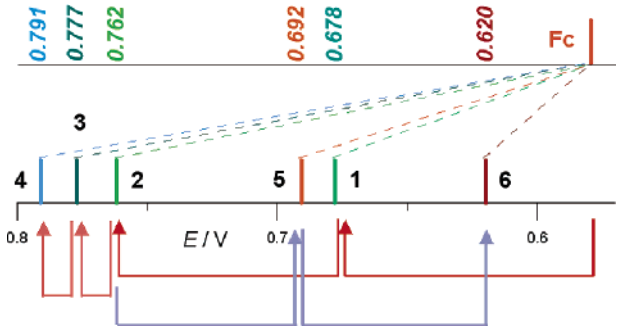

Figure 1. Comparison of the $E_{1/2}$ values (genetic diagram) for the reversible one-electron oxidation, localized in the ferrocenyl unit of all the compounds. Arrows indicate the additive effects of the heterocyclic substituents (see text).

In the positive potential region, all compounds show a single reversible one-electron process, localized onto the ferrocenyl unit. The $E_{1/2}$ values measured for species **1**−**6** and for pristine ferrocene are reported in Table 1 and graphically compared in Figure 1. In all cases, substitution onto the cyclopentadienyl ring(s) brings about a significant shift of ferrocenyl-based oxidation toward more positive potentials.

Such an effect is found to be additive: the stronger the electron-withdrawing properties of the substituents, the larger the potential shift. This suggests a strong electronic coupling between the two moieties in the ground state.

As matter of fact, the presence of a single pyridine ring (4-py) in **1** causes a positive shift of ferrocene-based oxidation with respect to ferrocene (Fc) by 98 mV, while in **2** (with two 4-py substituents) a 182 mV shift is measured (Figure 1). Furthermore, within a series of homologous disubstituted compounds, the addition of each N atom in hetero rings contributes ca. 15 mV to the overall potential shift with respect to Fc (182, 197, and 211 mV in **2**−**4**, respectively). This is in line with the known stronger electron-withdrawing properties of pyrimidine (5-pym) with respect to pyridine. Also the effect, due to bridging groups, between the ferrocenyl moiety and the N hetero ring was investigated by comparing the redox properties of species **2**, **5**, and **6**, where a phenyl ring is interposed between the ferrocenyl moiety and the 4-py rings. Despite the fact that phenyls are themselves slightly electron-withdrawing groups, their presence is found to shield effectively the electronic interaction between ferrocenyl and 4-py groups: this results in a significant shift to less positive potentials of the ferrocenyl-based oxidations in **5** and **6** with respect to **2** (by 71 and 141 mV, respectively). Additive effects of ligands on the redox potential were similarly observed and parametrized for several coordination and organometallic compounds.[11]

The identification of anodic processes as oxidations of the ferrocenyl moiety in all species is straightforward, as was also suggested by DFT calculations.[12] Despite the fact that the ferrocenyl and hetero ring moieties interact quite strongly with each other, a description of their redox properties in terms of a mainly localized redox orbital model is viable. The HOMO and LUMO surfaces of **5** and **2**, shown in Figure 2, are adequate representatives of those of the whole family of complexes. No substantial difference is highlighted as to the HOMOs of the various complexes; a very good linear correlation between the calculated HOMO energy and the corresponding oxidation potential for all complexes was found (see Figure S1 in the Supporting Information), confirming that the greater HOMO stabilization is responsible for the increasingly difficult oxidation.[14] In contrast, the complexes can be classified into two different groups on the basis of the LUMO structure: (i) the asymmetric complexes (**1**, **3**, **5**), characterized by a LUMO mainly localized upon one specific ligand, and (ii) the symmetric ones (**2**, **4**, **6**) in which the LUMO is largely delocalized over the two identical ligands.

In view of the aforementioned properties of LUMOs, the reduction behavior of complexes **1**−**6** is expectedly more complex than the oxidation one. All species, except **1**, show two or more one-electron-reduction processes in the negative potential region, as shown in Figure 3. In the case of **1**, only a single one-electron reversible reduction process ($E_{1/2} = -2.40$ V; see Figure 3a, dashed line) is observed, largely localized on the 4-py (pyridyl-centered LUMO). The injection of a second electron, either coupling with the first one within the same LUMO or entering the second unoccupied MO (2-LUMO), is likely to occur at much higher energy and is therefore unaccessible within the experimental potential window (∼−3.2 V).

In the case of **2**, in fact, two subsequent one-electron reductions (Figure 3a, solid line) are observed, separated by a relatively large potential gap (400 mV). The first reduction peak ($E_{1/2} = -2.24$ V) appears at lower energies than in **1**, as expected for the more delocalized LUMO (Figure 2d). The second reduction peak is not fully reversible, since it displays an anodic-to-cathodic peak ratio ($i_{p,a}/i_{p,c}$) much lower than that at any scan rates up to 50 V/s. However, when the scan rate is increased, the peak potential was found to shift toward more negative potentials by ca. 30 mV/decade, thus suggesting that the observed irreversibility may be due

(11) (a) Lever, A. B. P. *Inorg. Chem.* **1990**, *29*, 1271. (b) Lu, S.; Strelets, V. V.; Ryan, M. F., Pietro, W. J.; Lever, A. B. P. *Inorg. Chem.* **1996**, *35*, 1013. (c) Guedes da Silva, M. F. C.; Trzeciak, A. M.; Ziólkowski, J. J.; Pombeiro, A. J. L. *J. Organomet. Chem.* **2001**, *620*, 174. (d) Treichel, P. M.; Durren, G. E.; Mueh, H. J. *J. Organomet. Chem.* **1972**, *44*, 339.

(12) Geometry optimizations were carried out for all species with 6-31G*, basis set[13a−c] and hybrid functional B3LYP,[13d,e] using Spartan 02.[13f] The calculated gas-phase molecular structures are in excellent agreement with those from X-ray determinations.[5]

(13) (a) Hehre, W. J.; Ditchfield, R.; Pople, J. A. *J. Chem. Phys.* **1972**, *56*, 2257. (b) Hariharan, P. C.; Pople, J. A. *Theor. Chim. Acta* **1973**, *28*, 213. (c) Rassolov, V.; Pople, J. A.; Ratner, M.; Windus, T. L. *J. Chem. Phys.* **1998**, *109*, 1223. (d) Becke, A. D. *J. Chem. Phys.* **1993**, *98*, 5648. (e) Lee, C.; Wang, W.; Parr, R. G. *Phys. Rev. B* **1988**, *37*, 785. (f) Spartan 02; Wavefunction, Inc.

(14) Sarapu, A.; Fenske, R. F. *Inorg. Chem.* **1975**, *14*, 247.

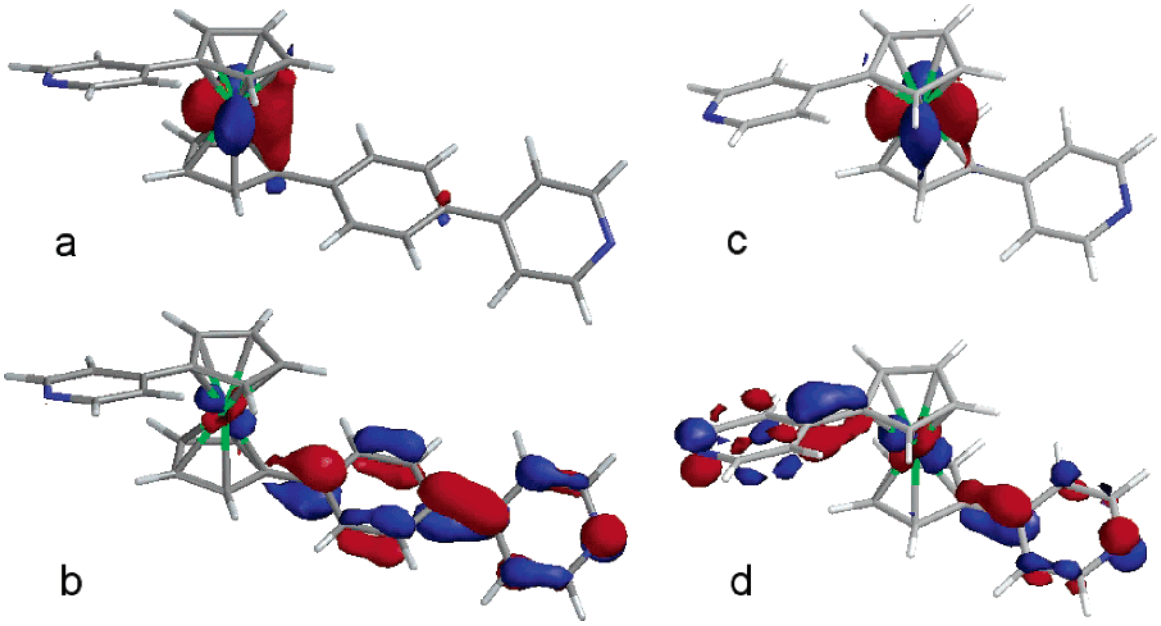

Figure 2. Molecular orbital surfaces showing the localization of the first orbitals involved in the redox process of (a) the HOMO of **5** centered on the ferrocenyl unit, (b) the LUMO of **5** mainly localized on the phenyl−pyridine ligand, (c) the HOMO of **2** localized on the metal center, and (d) the LUMO of **2** delocalized between the two pyridine ligands.

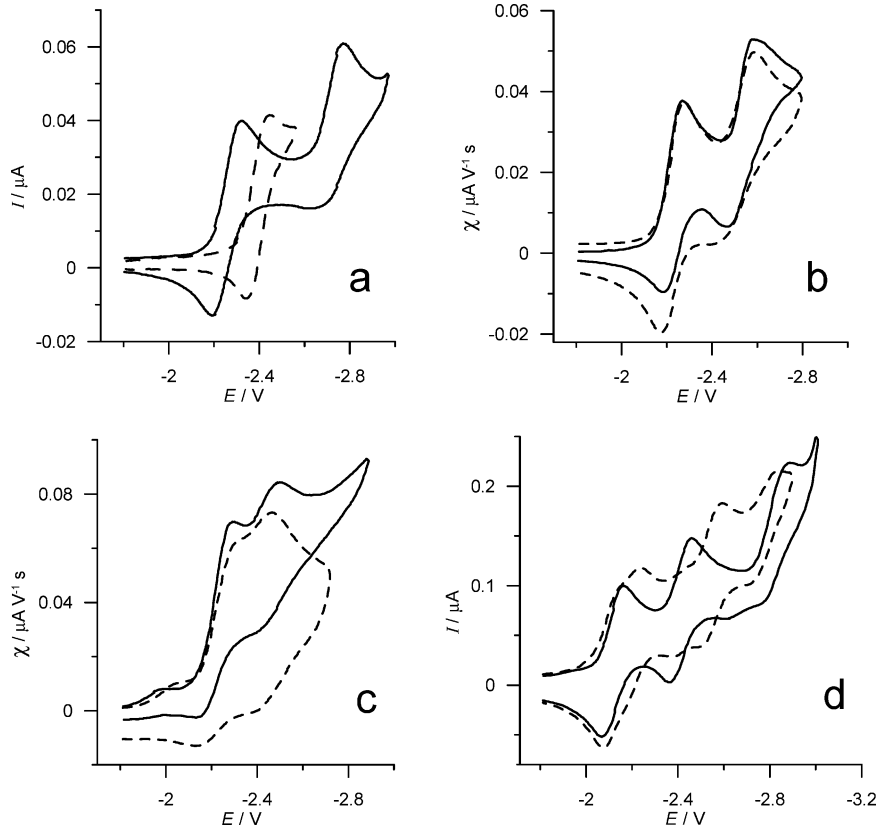

Figure 3. Cyclic voltammetric curves in THF solutions (0.05 M TBAH, at $T = 295$ K, working electrode Pt disk (125 μm) and scan rate 1 V s^{-1}) of (a) 0.7 mM **1** (dashed line) and 0.7 mM **2** (solid line), (b) 0.8 mM **3** (dashed line: CV curve at 50 V s^{-1}), (c) 1.1 mM **4** (dashed line: CV curve at 10 V s^{-1}), and (d) 0.9 mM **5** (solid line) and 0.9 mM **6** (dashed line). Potentials are referenced to SCE.

to a follow-up chemical reaction coupled to the reduction process (EC mechanism[15]). The digital simulation of the CV curve, calculated according to such a mechanism, allowed us to estimate the rate constant of the chemical step (≥50 s^{-1}) and the standard potential of the second reduction process (Table 1).

A similar behavior was found for **3**: the CV curve displays two quasi-reversible one-electron reductions (Figure 3b). The first process occurs at −2.22 V, a few

(15) Bard, A. J.; Faulkner, L. R. *Electrochemical Methods: Fundamentals and Applications*; Wiley: New York, 2001; Chapter 12 and pp 200−201.

tenths of a millivolt less negative in potential than in **2**, which is consistent with the slightly lower LUMO energy; it mainly involves the pyrimidine group (see Figure S2 in the Supporting Information). This is in line with the stronger electron-withdrawing effect of 5-pym with respect to 4-py, as found from the analysis of the ferrocene-based oxidations. Interestingly, the second reduction of **3** occurs at significantly less negative potentials than in **2** and the potential separation between the first and second reductions narrows by about 100 mV in **3** with respect to **2**. The MO calculations agree with experimental findings, as the energy separation between LUMO and 2-LUMO in **3** is much lower than in **2**. The LUMO of $[\mathbf{3}]^-$ is widely delocalized upon both of the ligands (see Figure S3 in the Supporting Information).[16]

A significantly narrower separation between the two subsequent reduction peaks was found in complex **4** (Figure 3c). However, in this case the CV curve exhibits a highly irreversible pattern, with an $i_{p,a}/i_{p,c}$ ratio $\ll 1$ at any scan rate (up to 50 V/s) for both reduction peaks. At high scan rates (Figure 3c, dashed line), the reversibility of the second peak increases while little or no effect was found on the first peak. Such a CV behavior suggests that the first one-electron-reduction process in **4** may trigger a follow-up chemical reaction, yielding a novel species that is in turn responsible for the second reduction peak, according to an ECE mechanism.[17]

The insertion of phenyl spacers between hetero rings and the ferrocenyl moiety increased the stability of electrochemically generated anions. In fact, complexes **5** and **6** undergo two subsequent fully reversible one-electron reductions that were attributed to the phenyl−pyridine unit and to the (phenyl−)4-py one. The peaks are significantly shifted with respect to the previous complexes toward less negative potentials (see Table 1), as a consequence of the increased delocalization of the LUMOs allowed by the close-to-coplanar geometry adopted by the rings (Figure 2b). The second 4-py-centered reduction in **5** occurs at the same potential as in **1**, suggesting that, in **5**, the two ligands are in fact only weakly interacting with each other. Little or no interligand interaction is also evidenced in **6**: the two subsequent reductions are nearly superimposed in a single reduction peak, with a potential separation of ca. 110 mV (Figure 3d, dashed line, and Table 1). This is in line with the fact that the LUMO and 2-LUMO, both linear combinations of the phenyl−pyridine-based MOs, are nearly degenerate because of the very weak communication between the two ligands.

The anticipation of the first two reductions in **5** and **6**, consequent to the stabilization of the respective LUMOs, allows us to observe further reduction processes of both complexes. Nevertheless, the third reduction was associated in both cases with a follow-up chemical reaction responsible for $i_{p,a}/i_{p,c} < 1$ and for the occurrence of a small additional oxidation peak in the reverse scan (located at −2.62 and −2.39 V for **5** and **6**, respectively). Finally, **6** also undergoes a fourth reduction process within the experimental potential window, not observed for **5**. The separation between second and third reduction peaks (460 mV in **5** and 340 mV in **6**) is significantly larger than that between the first two peaks (290 and 110 mV, respectively), thus suggesting that the third process (and also the fourth one in **6**) may correspond to the coupling of a second electron in the same redox orbital(s) involved in the first set of reductions.[8]

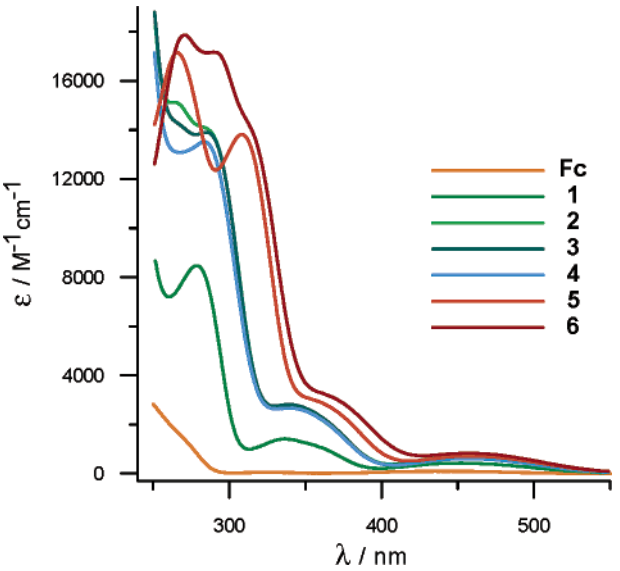

Figure 4. Electronic absorption spectra of the whole class of compounds in THF (T = 295 K).

Table 2. UV−Vis Absorption Spectroscopic Data[a]

compd	λ_{max}/nm ($\epsilon \times 10^{-3}$/M^{-1} cm^{-1})			
Fc			325 (0.06)	440 (0.10)
$[Fc]^+$	254 (7.20)	285 (5.50)		618 (0.18)
1		279 (8.50)	337 (1.44)	452 (0.44)
2	265 (15.1)	285 sh (14.1)	339 (2.81)	460 (0.79)
$[\mathbf{2}]^+$	273 (19.7)	314 (11.3)	429 (2.88)	516 (2.14)
3		285 (13.9)	340 (2.80)	459 (0.69)
4		284 (13.5)	341 (2.69)	458 (0.62)
5	266 (17.1)	309 (13.8)	359sh (3.56)	459 (0.71)
6	271 (17.9)	291 (17.2)	365sh (3.20)	459 (0.84)

[a] Data measured in THF at 295 K.

Electronic Absorption Spectra and Spectroelectrochemistry. Electronic absorption spectra of species **1**−**6**, in the range 250−550 nm, are compared in Figure 4, and the relevant data are gathered in Table 2.

Any perturbation of the electronic structure of ferrocene brings about a bathochromic shift of UV−vis transitions. In fact, ferrocene exhibits two weak bands at 325 and 440 nm, assigned to d−d transitions, which shift to lower energy (by about 20 nm) upon substitution with conjugated electron-withdrawing groups. In addition, all spectra show major absorption bands in the range 265−310 nm that are assigned to the intraligand $\pi \rightarrow \pi^*$ transitions of nitrogen-containing ligands (L), probably overlapped with the $d\pi(Fe) \rightarrow \pi^*(Cp-L)$ bands.[18] Such absorption bands are not observed in the case of Fc.

(16) The second reduction peak is not fully reversible, since $i_{p,a}/i_{p,c}$ was lower than 1 at scan rates as high as 50 V/s. At the same time, the cathodic-to-anodic peak potential separations increased with scan rate (see Figure 3b, dashed line), suggesting slow electron-transfer kinetics. The digital simulation of the CV curve, calculated according to such a hypothesis, showed in fact a rather good agreement with the experimental curve using the standard ET rate constant $\sim 10^{-2}$ cm s^{-1}. The slow ET kinetics might be associated with the molecular rearrangement coupled to the reduction of the radical monoanion, such as an increase of coplanarity (Figures S2 and S3 in the Supporting Information). Further investigations are currently in progress to identify the nature of such a molecular reorganization.

(17) (a) Cattarin, S.; Ceroni, P.; Guldi, D. M.; Maggini, M.; Menna, E.; Paolucci, F.; Roffia, S.; Scorano, G. *J. Mater. Chem.* **1999**, *9*, 2743. (b) Zi-Rong, Z.; Evans, D. H. *J. Am. Chem. Soc.* **1999**, *121*, 2941.

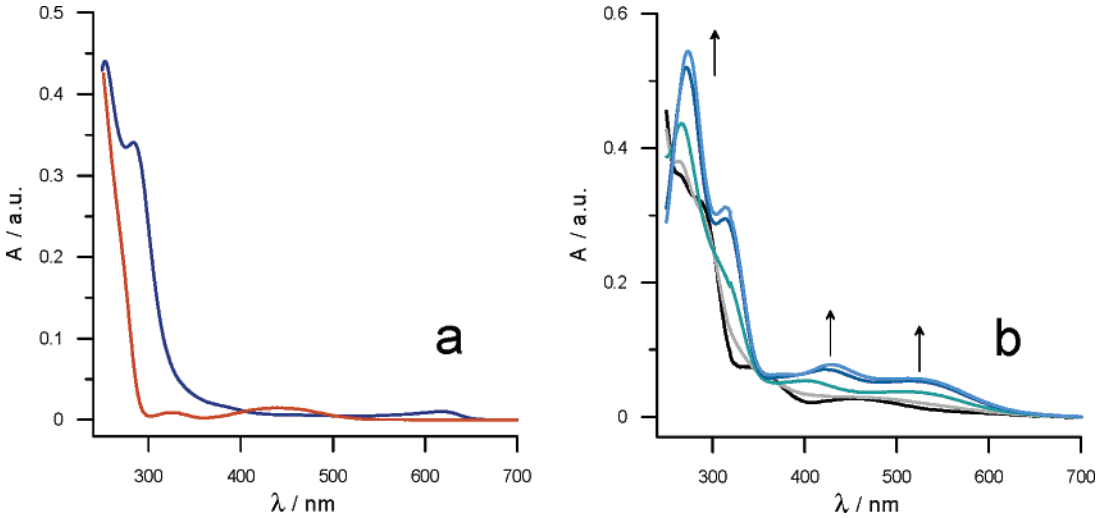

Figure 5. Electronic absorption spectra recorded at 295 K in THF (a) of Fc (orange line) and [Fc]+ (blue line) and (b) during oxidation of **2** to $[\mathbf{2}]^+$.

The small red shifts observed for **1**−**6** with respect to Fc are indicative of the weak electronic interaction between the hetero rings and the ferrocenyl moiety. On the other hand, such an interaction is strong enough to bring about a remarkable increase of intensity of the dπ(Fe) → π^*(Cp−L) absorption bands (compare the relative extinction coefficients in Table 2), likely because of the mixing of L orbitals and metal d orbitals that makes these symmetry-forbidden transitions more allowed.[19]

Finally, the spectroelectrochemical behavior of **2** was examined in the range 250−1000 nm (Figure 5b). Upon oxidation of **2** to $[\mathbf{2}]^+$, corresponding to the metal-centered oxidation of Fe(II) to Fe(III), two intense transitions appear at 429 and 516 nm. These are likely to be LMCT transitions that become possible due to the hole in the metal-based HOMO.[20] At higher energy, the oxidation generates a UV absorption pattern typical of the ferrocenium ion, $[Fc]^+$ (compare the blue trace in Figure 5a with the light blue trace in Figure 5b): two sharp bands at 273 and 314 nm, assigned to the intraligand $\pi \rightarrow \pi^*$ transitions of Cp overlapped with those of L. These transitions occur at lower energy than in $[Fc]^+$, according to the higher stability of involved orbitals caused by ligand substitutions. Moreover, this bathochromic shift is comparable to that observed above on comparing the spectra of Fc and complexes **1**−**6**. Similar results were also obtained for all the other complexes.

Conclusions

In summary, we have investigated the electronic properties of a number of pyridyl− and pyrimidyl−ferrocenyl ligands, aiming to develop a new class of photo- and/or electroactive complexes to be used in the assembly of redox-active supramolecular systems or coordination networks.[21] In the case of complexes **1**−**6** a strong electronic communication occurs between ferrocenyl and ligand moieties in the ground state. This is a useful prerequisite in the preparation of systems where intramolecular charge transfer is sought. For instance, the utilization of complexes **1**−**6**, as ligands in the formation of heterometallic *complexes of complexes* or coordination networks, is expected to lead to interesting collective properties, such as those sought in organometallic crystal engineering and molecular materials chemistry.[22] The convolution of the electrochemical behavior of **1**−**6** with the redox properties of metal centers will provide access to the physical chemistry of mixed-valence (and mixed-spin) supramolecular complexes. As an initial attempt in this direction, we have recently reported the successful preparation of metallamacrocycles of Cu(II), Cd(II), Zn(II), and Ag(I) by reacting transition-metal salts with the ferrocenyl ligand **1**.[5c] The investigation of their electrochemical properties is under way. In addition, all species display stability to heat and light, and this could open the door to developing applications in the area of molecular devices.

In addition, once more we have demonstrated the concept that electrochemical potentials are additive with respect to ligand substitution and a very effective modulation of electronic properties can be obtained by a suitable choice of heterocycle.

Acknowledgment. We thank the MIUR (PRIN 2002035735 (D.P., F.P., M.M., and C.B.); FIRB projects RBAU01NAKK2 (D.B., F.G., and M.P.)) and the University of Bologna for financial support.

Supporting Information Available: Figures S1−S3, giving HOMO energies vs oxidation potentials for the whole family of complexes, the molecular orbital surface of **3**, and the LUMO surface of **3**, respectively. This material is available free of charge via the Internet at http://pubs.acs.org.

OM049212L

(18) (a) Numes, C. D.; Santos, T. M.; Carapuça, H. M.; Hazell, A.; Pillinger, M.; Madureire, J.; Xue, W.-M.; Kühn, F. E.; Gonçalves, I. S. *New J. Chem.* **2002**, *26*, 1384. (b) Xue, W.-M.; Kühn, F. E.; Herdtweck, E.; Li, Q. *Eur. J. Inorg. Chem.* **2001**, 213.

(19) Das, A.; Bajaj, H. C.; Bhadbhade, M. M. *J. Organomet. Chem.* **1997**, *544*, 55.

(20) Siu-Ming, L.; Marcaccio, M.; McCleverty, J. A.; Ward, M. D. *Chem. Mater.* **1998**, *10*, 3272.

(21) (a) Moulton, B.; Zaworotko, M. J. *Chem. Rev.* **2001**, *101*, 1629. (b) Carlucci, L.; Ciani, G.; Proserpio, D. M. *Cryst. Eng. Commun.* **2003**, *5*, 269. (c) Kitagawa, S.; Kitaura, R.; Noro, S. *Angew. Chem., Int. Ed.* **2004**, *116*, 2388. (d) Janiak, C. *Dalton* **2003**, 2781.

(22) (a) Haiduc, I.; Edelmann, F. T. *Supramolecular Organometallic Chemistry*; Wiley-VCH: Weinheim, Germany, 1999. (b) Steed, J. W.; Atwood, J. L. *Supramolecular Chemistry*; Wiley: New York, 2000. (c) Braga, D. *Chem. Commun.* **2003**, 2751.